Bych K1, Netz DJ, Vigani G, Bill E, Lill R, Pierik AJ, Balk J.The essential cytosolic iron-sulfur protein Nbp35 acts without Cfd1 partner in the green lineage. Journal of Biological Chemistry volume 283 fascicolo 52, anno 2008, pagg 35797-804. doi: 10.1074/jbc.M807303200

Abstract
In photosynthetic eukaryotes assembly components of iron-sulfur (Fe-S) cofactors have been

studied in plastids and mitochondria, but how cytosolic and nuclear Fe-S cluster proteins are assembled is not known. We have characterized a plant P loop NTPase with sequence similarity to Nbp35 of yeast and mammals, a protein of the cytosolic Cfd1-Nbp35 complex mediating Fe-S cluster assembly. Genome analysis revealed that *NBP35* is conserved in the green lineage but that *CFD1* is absent. Moreover, plant and algal NBP35 proteins lack the characteristic C*XX*C motif in the C terminus, thought to be required for Fe-S cluster binding. Nevertheless, chemical reconstitution and spectroscopy showed that *Arabidopsis* (At) NBP35 bound a [4Fe-4S] cluster in the C terminus as well as a stable [4Fe-4S] cluster in the N terminus. Holo-AtNBP35 was able to transfer an Fe-S cluster to an apoprotein *in vitro*. When expressed in yeast, AtNBP35 bound ^{55}Fe dependent on the cysteine desulfurase Nfs1 and was able to partially rescue the growth of a *cfd1* mutant but not of an *nbp35* mutant. The *AtNBP35* gene is constitutively expressed in planta, and its disruption was associated with an arrest of embryo development. These results show that despite considerable divergence from the yeast Cfd1-Nbp35 Fe-S scaffold complex, AtNBP35 has retained similar Fe-S cluster binding and transfer properties and performs an essential function.
Previous Section
Next Section
Proteins carrying iron-sulfur (Fe-S) clusters as cofactors are common in virtually all life forms. Fe-S proteins catalyze crucial steps in fundamental processes, including nitrogen fixation, respiration, photosynthesis, various metabolic pathways, and regulation of gene expression (1). The most common types of Fe-S clusters are the [2Fe-2S] and the cubane [4Fe-4S] form. Although Fe-S clusters can be assembled by chemical means, dedicated proteins for *in vivo* Fe-S protein maturation have been discovered over the past 10 years (2, 3). In plants assembly proteins have been localized to the plastids and mitochondria, the endosymbiotic organelles where photosynthesis and respiration take place, respectively (for review, see Refs. 4–6). The plastids contain all six proteins of the so-called SUF system plus NFU-type scaffolds. The mitochondrial matrix contains the ISC[3] system (for iron-sulfur cluster assembly). Both systems appear to follow the same biochemical steps; (i) generation of persulfide by a cysteine desulfurase (the Nfs1-Isd11 complex in mitochondria; CpNifS in plastids), (ii) transfer of persulfide and combination with iron to form an Fe-S cluster on a scaffold protein (ISU proteins in mitochondria; NFU2 in plastids), (iii) transfer of the Fe-S cluster from the scaffold protein to a target protein (mediated by chaperones in the ISC system).

Important Fe-S enzymes are also found in the cytosol and nucleus (3, 4). In plants, these include DNA repair enzymes, RNA polymerase I and III (7), xanthine dehydrogenase, abscisic aldehyde oxidase (AAO3), and cytosolic aconitase. How these proteins obtain their Fe-S clusters is currently not known. By analogy with yeast, it is presumed that the mitochondria are required for cytosolic Fe-S cluster assembly, but supporting experimental evidence has not yet been provided. Bioinformatic analyses have revealed that sequence relatives of the yeast CIA proteins (for cytosolic iron-sulfur cluster assembly) are also present in the genomes of the model plant species *Arabidopsis thaliana* and the green alga *Chlamydomonas reinhardtii* (4, 8). In yeast and humans the CIA machinery includes two P-loop NTPases, Cfd1 and Nbp35, which form a heterotetrameric complex and function as Fe-S scaffolds, mediating the *de novo* assembly of an Fe-S cluster and its transfer to target apoproteins (9–12).
Cfd1 and Nbp35 are classified as Mrp-like proteins that belong to the Mrp/NBP35 subfamily of P loop NTPases (13). Although Cfd1 and Nbp35 share 49% sequence similarity, they can be distinguished as different types based on their N-terminal domains (Fig. 1*B*). A third type of Mrp-like protein, HCF101, was characterized in plastids and is involved in the assembly of Photosystem I, which has three [4Fe-4S] clusters (14, 15). Recently, we have identified a fourth type of eukaryotic Mrp-like protein associated with Fe-S protein assembly. This protein, named Ind1, is localized in the mitochondria and is required for the effective assembly of respiratory Complex I, which contains eight Fe-S clusters, in the yeast *Yarrowia lipolytica* (16).

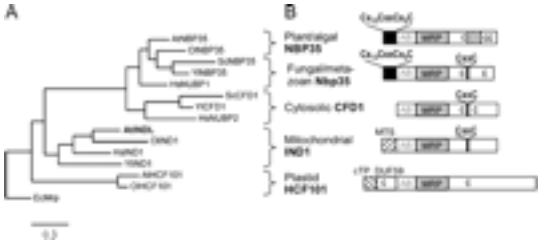

View larger version:

In this page In a new window

Download as PowerPoint Slide

FIGURE 1.

Plant and algal genomes contain NBP35 but not CFD1. *A*, phylogenetic analysis of Mrp-like proteins in eukaryotes. Protein sequences containing the Mrp family signature in the model plant *A. thaliana* (*At*), the green alga *Ostreococcus lucimarinus* (*Ol*), the fungi *S. cerevisiae* (*Sc*), and *Y. lipolytica* (*Yl*) and man (*Hs*) were aligned with T-COFFEE. Tree building and tree rendering were performed with PhyML and TreeDyn, respectively, based on the central portion of the proteins (including the Walker AB motifs and the Mrp domain). *E. coli* (*Ec*) Mrp served as an out-group. *B*, diagrams of the Mrp-like proteins showing domain structure and conserved motifs. Plant/algal NBP35 proteins have a C-terminal insertion of conserved sequence not found in other groups (wave pattern). *AB*, Walker A and B motifs; *MRP*, Mrp family signature (InterPro IPR000808); *C*, (semi)conserved cysteine residues; *MTS*, mitochondrial targeting signal; *cTP*, chloroplast transit peptide; *DUF59*, domain of unknown function 59 (InterPro IPR002744).

To initiate studies on Fe-S protein assembly in the plant cytosol and analyze how this process may depend on the organellar assembly systems, we investigated two uncharacterized Mrp-like proteins in *Arabidopsis*. Here we show that NBP35 (gene locus At5g50960) is essential for embryo development and is localized in the cytosol, whereas the gene product of At4g19540, designated INDL for Ind1-like, was localized in the mitochondria. AtNBP35 bound [4Fe-4S] clusters that were readily transferred to an apoprotein *in vitro*, consistent with an Fe-S scaffold function.

Previous Section
Next Section

EXPERIMENTAL PROCEDURES

Plant Material and Yeast Strains—The *A. thaliana* lines, SALK_054678 and SALK_056204, were obtained from the Nottingham Arabidopsis Stock Centre. The presence and position of the T-DNA insert in the *NBP35* gene (At5g50960) was confirmed by PCR. Segregation analysis showed that the T-DNA was linked to the embryo lethality phenotype in the SALK_056204 line. *Arabidopsis* cell cultures were generated as described (17). *Saccharomyces cerevisiae* strain W303-1A (*MATa, ura3-1, ade2-1, trp1-1, his3-11,15, leu2-3112*) served as wild type. The Gal-NFS1 strain and conditions for depletion of Nfs1 protein were described previously (18). The following yeast plasmids were used: pRS416 (p416) containing the *MET25* promoter for intermediate expression and pRS426 (p426) with the *TDH3* promoter for high expression (19).

Cell Fractionation and Protein Blot Analysis—*Arabidopsis* cell cultures were used as source material to obtain highly purified mitochondria (20), nuclei (21), and a cytosolic fraction. For the latter, drained cells were squashed in one volume of cold nuclei isolation buffer (21) and centrifuged for 10 min at 13,000 × *g*, and the supernatant was collected. Chloroplasts were isolated from rosette leaves (22). Total protein extract from plant tissue was prepared by grinding the tissue with 1–2 volumes of cold 50 mM Tris-HCl, pH 8.0, 5% (v/v) glycerol, 1% (w/v) SDS, 10 mM EDTA, and 1 mM phenylmethanesulfonyl fluoride followed by centrifugation at 13,000 × *g* for 15 min to remove cell debris. Protein concentrations were determined with Coomassie Dye Reagent (Bio-Rad). Thirty μg of protein was separated by SDS-PAGE, blotted, and labeled with antibodies following standard protocols.

Polyclonal antibodies were raised against purified His-AtNBP35 and His-AtINDL. Antibodies

against AtISU1 were a kind gift from Stéphane Lobréaux (23), and antibodies against pea PETC were kindly provided by John C. Gray (24). The monoclonal antibody against *Arabidopsis* actin (MA1–744) was from Affinity BioReagents, Golden, CO; polyclonals against histone 3 (ab1791) were from Abcam, Cambridge, UK. Antisera against Nfs1 and Leu1 were described previously (18).

In Vitro Fe-S Analysis—The full-length (FL) *AtNBP35* coding sequence or a version lacking the first 54 codons (ΔN) was isolated from wild-type *Arabidopsis* cDNA and cloned into the pET15b expression vector (Novagen) in-frame with an N-terminal His tag. Protein overexpression and affinity purification were carried out following the manufacturer's manuals. Chemical reconstitution of the Fe-S clusters was carried out in an anaerobic chamber (Coy Laboratory Products, Ann Arbor, MI). In a typical experiment, 20–30 μM protein in 25 mM Tris-HCl, 150 mM NaCl, pH 8.0 (buffer A), was treated with 10 mM dithiothreitol (final concentration) at 15 °C for 1 h. The reconstitution was started by the addition of 10 mol eq of ferric ammonium citrate and Li_2S followed by incubation at 15 °C for 3 h. To remove non-bound iron and sulfide, reconstituted AtNBP35 was passed through a Sephadex G25 gel filtration column using buffer A containing 1 mM dithiothreitol. The assembly of Fe-S clusters was ascertained by UV-visible spectroscopy (Jasco V-550). The quantification of iron and acid-labile sulfide and performance of *in vitro* cluster transfer assays were as previously described (11, 25).

Electron Paramagnetic Resonance (EPR) and Mössbauer Spectroscopy—Protein samples were reconstituted as described above. Low temperature X-band EPR spectra of samples reduced with 2 mM dithionite were recorded with a Bruker ESP 300E cw spectrometer equipped with a helium flow cryostat ESR910 (Oxford Instruments). For the preparation of Mössbauer samples reconstitution was carried out with $^{57}FeSO_4$. The samples were concentrated with Vivaspin 30-kDa concentrator devices and frozen on a cold aluminum block in the anaerobic glove box. Mössbauer measurements and simulations were carried out as described in Barthelme *et al.* (26).

Miscellaneous Methods—Published methods used were transient expression of green fluorescent protein (GFP) fusion protein using vector pOL-GFP-S65C (27) and radiolabeling of yeast cells, protein extraction, and immunoprecipitation (18). Error bars represent the S.D. value.

Previous Section
Next Section

RESULTS

NBP35 but Not CFD1 Is Conserved in the Green Plant Lineage—With the availability of recently sequenced genomes of plants and algae, we investigated the conservation of Mrp-like proteins and their domains in the green lineage. Three separate coding sequences for proteins with a Mrp family signature were usually found: one with a putative mitochondrial targeting sequence, designated INDL, the plastid HCF101, characterized by an N-terminal DUF59 domain, and an NBP35 homolog with an N-terminal Fe-S cluster domain (Fig. 1). No other sequence relative that could correspond to yeast Cfd1 was found in any of the six plant, one moss, and four green algal genomes analyzed. In addition, the predicted NBP35 proteins in the green lineage differed from those in the fungi/Metazoa group in the C-terminal region after the highly conserved VENMS motif (Fig. 1*B* and supplemental Fig. S1). Most notably, the C-terminal C*XX*C motif, which is critical for Fe-S cluster binding to Cfd1 and Nbp35 in yeast,[4] is absent from plant and algal NBP35 proteins. Instead, a ~35-amino acid insertion is found that is conserved in all Viridiplantae genomes investigated so far but that has no sequence similarity to other known protein motifs. As a consequence, only one C-terminal cysteine residue is conserved in all NBP35 proteins: Cys-234 in *S. cerevisiae* numbering, corresponding to Cys-220 in *Arabidopsis* NBP35. However, a number of semiconserved cysteine residues are found in the C-terminal 70-amino acid sequence of plant and algal NBP35 proteins. The absence of *CFD1* genes in the green lineage suggests that the NBP35 protein may function as a homo-oligomer in the cytosol without a CFD1-like partner.

AtNBP35 Is a Soluble Cytosolic Protein—To determine the cellular localization of NBP35 (At5g50960) in the model plant *Arabidopsis*, the full coding sequence isolated from cDNA was

fused in-frame to a C-terminal GFP sequence and transiently expressed using particle bombardment of *Arabidopsis* leaves. GFP fluorescence was found in the cytoplasm, which is appressed to the plasma membrane in the highly vacuolate, jigsaw-shaped epidermal cells (Fig. 2, *A* and *B*). Green fluorescence was also observed in the nucleus, which, however, may be due to diffusion, a recurrent problem in determining the localization of nuclear proteins as GFP fusions (28, 29). We, therefore, investigated the localization of endogenous AtNBP35 using cell fractionation and immunoblotting. Antibodies specific to AtNBP35 (see supplemental Fig. S2) recognized an ~37-kDa protein in total plant extracts (Fig. 2*C*), in agreement with the predicted molecular mass of 37,306 Da. The AtNBP35 protein was found in the soluble, cytosolic fraction but not in purified nuclei, mitochondria, or chloroplasts. We also investigated the localization of the INDL protein (At4g19540) using specific antibodies and obtained a signal in the purified mitochondrial fraction only, similar to the pattern observed for ISU1 (Fig. 2*C*). Note that these two proteins are not or are barely detectable in total extract due to their low abundance and the relatively minor contribution of mitochondria to total protein in plant extract. These data show that AtNBP35 is a soluble cytosolic protein that is spatially separated from the homologous AtINDL protein in the mitochondria.

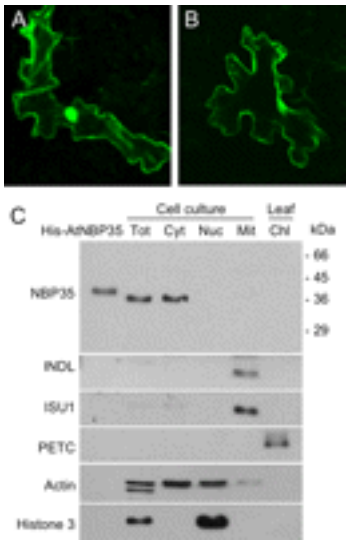

View larger version:

In this page In a new window

Download as PowerPoint Slide

FIGURE 2.

***Arabidopsis* NBP35 is localized in the cytosol.** *A* and *B*, the fusion gene *AtNBP35-GFP* was placed under the control of the 35S promoter and transiently expressed in *Arabidopsis* leaves using particle bombardment. Images of epidermal cells expressing GFP were obtained by confocal microscopy. *C*, immunolocalization of NBP35 and INDL in *Arabidopsis* cell fractions. Total proteins (*Tot*), cytosolic fraction (*Cyt*), and purified nuclei (*Nuc*), mitochondria (*Mit*), or chloroplasts (*Chl*) were separated by SDS-PAGE (30 μg of protein per lane) and labeled with specific antibodies. The purity of the cell fractions was verified with antibodies against the following marker proteins: mitochondrial Fe-S scaffold protein (*ISU1*), Rieske protein of the cytb_6f complex in chloroplasts (these organelles are not developed in cell culture; therefore, no signal is seen in total protein extract) (PETC), actin (cytosol/nuclear envelope) and histone 3 (nucleus).

Both the N- and C-terminal Domains of AtNBP35 Bind Fe-S Clusters—Because the characteristic C-terminal C*XX*C motif of the Cfd1/Nbp35 scaffold proteins is missing in plant and algal NBP35 proteins, it was of interest to analyze the capacity of the C-terminal domain to bind an Fe-S cluster. To this end, AtNBP35 was overproduced in *Escherichia coli*, either FL or lacking the N-terminal Fe-S cluster binding motif (ΔN). The proteins were purified by His-tag affinity purification (Fig. 3*A,*

inset). The FL protein appeared brown in color, whereas the ΔN protein was virtually colorless except for a light yellow hue. UV-visible spectroscopy of the FL protein showed absorbance peaks at 320 and 415 nm, which were more than halved upon addition of dithionite (Fig. 3*A*). These spectral features are characteristic of a [4Fe-4S] cluster (30); however, the intensity of the signal indicated that only a minor fraction of the molecules contained a cluster (11). The UV-visible spectrum of ΔN AtNBP35 (as isolated) did not have a pronounced absorbance. We, therefore, incubated both FL and ΔN protein with excess iron and sulfide under reductive, anaerobic conditions to chemically reconstitute the Fe-S clusters. Quantification of protein-bound Fe and sulfide showed that FL AtNBP35 bound 5.7 ± 1.2 iron and 5.1 ± 0.8 acid-labile sulfide per polypeptide, whereas the ΔN protein bound 1.8 ± 0.7 iron and 1.7 ± 0.1 acid-labile sulfide per polypeptide (Fig. 3*B, inset*). Subtraction of these numbers indicate that the N-terminal domain bound a [4Fe-4S] cluster. The C terminus may bind either a [2Fe-2S] cluster or a [4Fe-4S] cluster bridging two polypeptides, assuming complete reconstitution in our samples. The second possibility is supported by the UV-visible spectrum of reconstituted ΔN AtNBP35 (Fig. 3*B*), which is typical of a cubane cluster. Further support for a cubane cluster was obtained by EPR spectroscopy, showing attenuation of the EPR signal of the reduced protein above 40 K (supplemental Fig. S3).

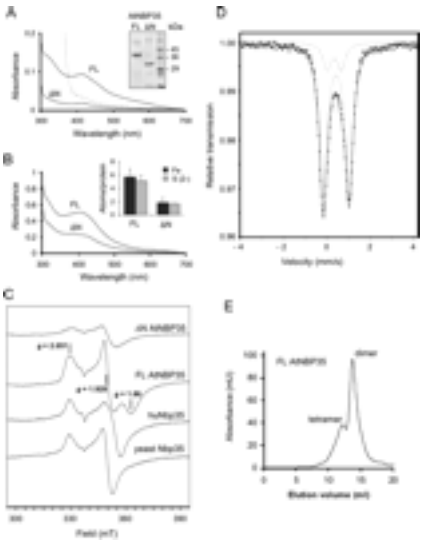

View larger version:

In this page In a new window

Download as PowerPoint Slide

FIGURE 3.

AtNBP35 binds [4Fe-4S] clusters. *A*, UV-visible spectra of FL AtNBP35 and of AtNBP35 lacking the N-terminal Fe-S cluster binding motif (ΔN). The His-tagged proteins were overproduced in *E. coli* and isolated by affinity chromatography. Spectra were recorded at protein concentrations of 28 μM (FL) and 47 μM (ΔN) and normalized to 25 μM for comparison. *Dashed line*, FL AtNBP35 reduced with 2 mM sodium dithionite. *Inset*, Coomassie staining of the purified protein samples separated by SDS-PAGE, showing only minor contaminating protein bands. *B*, UV-visible spectra of FL and ΔN AtNBP35 after reconstitution with sulfide and iron under anaerobic conditions. Spectra were recorded at protein concentrations of 20 μM (FL) and 31 μM (ΔN) and normalized to 25 μM for comparison. *Inset*, quantification of iron and acid-labile sulfide in reconstituted FL AtNBP35 ($n = 3$) and ΔN AtNBP35 ($n = 2$). *C*, comparison of the EPR signals of *Arabidopsis* NBP35, chemically reduced with 2 mM sodium dithionite, with the yeast and human Nbp35 proteins. EPR conditions: temperature, 10 K; microwave power, 2 milliwatts; microwave frequency, 9.459 GHz; modulation frequency, 100 kHz; modulation amplitude, 1.25 millitesla (*mT*). *D*, Mössbauer spectrum recorded at 80 K (no applied field) of reconstituted FL AtNBP35. The lines are the simulated quadrupole doublets with parameters (δ, ΔE_Q, full width at half-maximum, all in

mm/s): 0.43, 1.20, and 0.42 (85% of total intensity) and 0.34, 0.65, and 0.44 (15% of total intensity). The *solid line* is the sum of the simulated components. *E*, gel filtration of AtNBP35. His-tagged AtNBP35 (39.5 kDa) eluted in two peaks from a Superdex 200 column (GE Healthcare), corresponding to a dimeric form (calculated molecular mass of 98 ± 10 kDa) and a tetrameric form (188 ± 17 kDa).

The EPR spectrum of FL AtNBP35 after reduction with dithionite is rhombic and is dominated by the sharp signal of the N-terminal cluster, with g values of 2.051, 1.928, and 1.86 (Fig. 3*C*). In contrast, FL yeast Nbp35 and its human counterpart huNbp35 have an axial signal (Fig. 3*C*, see also Refs. 11 and 12). Comparison of the EPR signals of ΔN AtNBP35 (Fig. 3*C*) with the corresponding yeast ΔN Nbp35 and yeast Cfd1 (not shown) showed no pronounced differences for the relatively broad axial signal of the C-terminal domain. Mössbauer spectroscopy of the reconstituted protein (without reduction) showed that 85% of the iron associated with FL AtNBP35 was present in the form of $[4Fe\text{-}4S]^{2+}$ clusters (Fig. 3*D*). The values of the isomer shift (0.43 mm/s) and quadrupole splitting (1.20 mm/s) were similar to the values observed for delocalized mixed-valent ($Fe^{2.5+}$-$Fe^{2.5+}$) pairs in exclusively cysteine-coordinated $[4Fe\text{-}4S]^{2+}$ clusters (31). Because of the instability of ΔN AtNBP35 upon concentration of protein for Mössbauer spectroscopy, the individual isomer shift and quadrupole splitting parameters of N- and C-terminal clusters could not be determined.

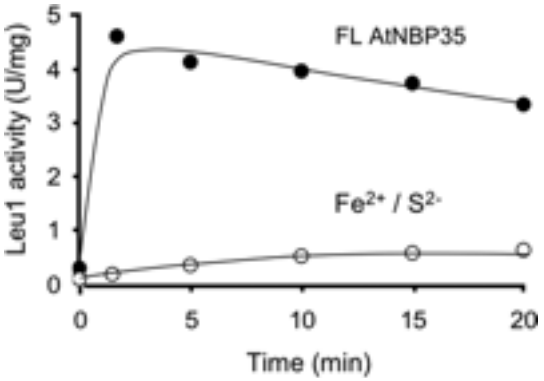

View larger version:

In this page In a new window

Download as PowerPoint Slide

FIGURE 4.

***In vitro* Fe-S cluster transfer from FL AtNBP35 to apoLeu1.** Reconstituted, FL AtNBP35 (2.4 μM, containing 13.2 μM Fe) was mixed with reduced apoLeu1 (4 μM) under anaerobic conditions, and Leu1 enzyme activity was measured at regular intervals (*closed circles*). As a control, activation of 4 μM apoLeu1 with 14.4 μM ferric ammonium citrate and Li_2S was carried out (*open circles*). Ferric ions are reduced to ferrous iron (Fe^{2+}) by Li_2S.

Gel filtration analysis of recombinant as isolated FL AtNBP35 showed that most of the protein occurred as a dimer, with some forming a tetramer (Fig. 3*E*). The chromatographic behavior of ΔN AtNBP35 or the reconstituted proteins could not be analyzed due to instability during the gel filtration procedure. Taken together, these data indicate that AtNBP35 occurs as a homo-oligomer with a stable [4Fe-4S] cluster in the N-terminal domain of each subunit and a C-terminal [4Fe-4S] cluster shared between two protomers.

Holo-AtNBP35 Can Transfer an Fe-S Cluster—Next we investigated whether the *Arabidopsis* NBP35 protein can act as an Fe-S scaffold in that it can transfer an Fe-S cluster to a potential target protein *in vitro*. Following a previously described assay (11), chemically reconstituted and desalted FL AtNBP35 was added to apoLeu1, the apoform of yeast isopropylmalate isomerase. Cluster transfer was followed by the generation of enzymatic activity upon conversion of apoLeu1

to the [4Fe-4S]-containing form. Cluster transfer to Leu1 occurred at a rate and efficiency comparable with that observed for yeast Nbp35 or the Cfd1-Nbp35 complex (11). At the earliest time point that we were able to measure (1.5 min), more than 80% of the maximal Leu1 activity was obtained. In contrast, chemical reconstitution with the same amounts of ferric iron and sulfide hardly led to activation of apoLeu1 (Fig. 4). The addition of 1 mM ATP/GTP (plus $MgCl_2$) had no effect on cluster transfer, as has been noted for ApbC (40) and Cfd1/Nbp35.[4] These *in vitro* data suggest that a labile Fe-S cluster of AtNBP35 can be donated to a target Fe-S protein.

AtNBP35 Binds Fe-S Clusters in Vivo but Cannot Replace Yeast NBP35—To analyze the physiological relevance of the *in vitro* data, we expressed *AtNBP35* in yeast cells (*S. cerevisiae, Sc*). First, we confirmed that the AtNBP35 protein was localized in the yeast cytosol (Fig. 5*A*). Second, we investigated whether Fe-S clusters were assembled on AtNBP35 by the yeast Fe-S cluster assembly machinery. For this we made use of a mutant, Gal-NFS1, containing a galactose-regulatable *NFS1* gene encoding the only cysteine desulfurase in yeast. Cluster assembly on AtNBP35 was followed by using a sensitive ^{55}Fe radiolabeling assay (18). In brief, yeast cells overproducing AtNBP35 were incubated with ^{55}Fe and washed followed by preparation of a soluble cell extract. AtNBP35 was immunoprecipitated from the cell extract and subjected to scintillation counting. A significant amount of ^{55}Fe (10 times over background) was associated with immunoprecipitated AtNBP35 (Fig. 5, *B* and *C*). Down-regulation of *NFS1* expression led to a near loss of ^{55}Fe bound to AtNBP35 (Fig. 5*C, last bar*). The Nfs1-dependent ^{55}Fe binding to AtNBP35 indicates that the iron was part of an Fe-S cluster.

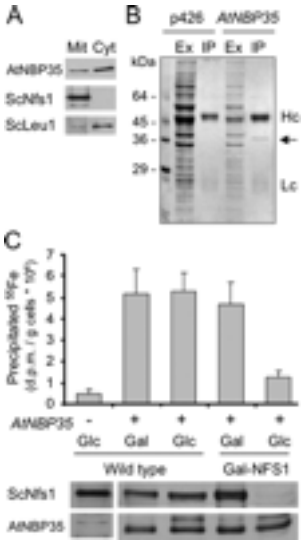

View larger version:

In this page In a new window

Download as PowerPoint Slide

FIGURE 5.

AtNBP35 binds an Fe-S cluster in the yeast cytosol. *A*, upon expression of AtNBP35 in yeast, the protein is localized in the cytosol. Yeast cells expressing *AtNBP35* from plasmid p426 were fractionated into mitochondria (*Mit*) and cytosol (*Cyt*) and subjected to immunoblot analysis to detect AtNBP35 protein, mitochondrial Nfs1, and cytosolic Leu1. *B*, AtNBP35 is specifically immunoprecipitated from yeast cell extracts. Yeast cells harboring an empty plasmid or a plasmid overexpressing *AtNBP35* were used to prepare a cell extract (*Ex*) for immunoprecipitation with anti-AtNBP35 agarose beads (*IP*). Equal amounts of extract and precipitated protein were separated by SDS-PAGE and stained with Coomassie. *Hc*, heavy chain; *Lc*, light chain. The *arrow* indicates immunoprecipitated AtNBP35. *C*, ^{55}Fe labeling and immunoprecipitation of AtNBP35 in wild-type and Gal-NFS1 yeast cells. Cells overproducing AtNBP35 were grown in the presence of glucose to down-regulate expression of *NFS1*, the gene for cysteine desulfurase. The ^{55}Fe associated with AtNBP35 was measured by scintillation counting. The amounts of AtNBP35 and

Nfs1 were visualized by immunoblotting (*lower panels*).

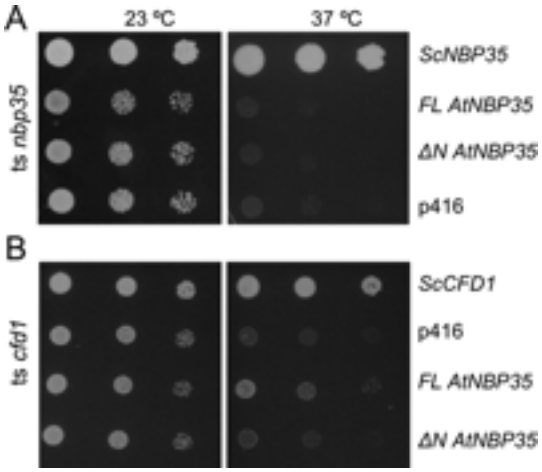

View larger version:

In this page In a new window

Download as PowerPoint Slide

FIGURE 6.

FL *AtNBP35* can partially rescue growth of a temperature-sensitive *cfd1* mutant in yeast, but not an *nbp35* mutant. *A*, growth of temperature-sensitive (*ts*) *nbp35* cells expressing FL or ΔN *AtNBP35*. Cells were transformed with a plasmid without insert (control, p416) or with a wild-type copy of yeast (*Sc*) *NBP35*, FL *AtNBP35*, or ΔN *AtNBP35*. Drops of 10-fold serial dilutions were spotted on solid SD medium with amino acids and grown at 23 °C or 37 °C. *B*, as in *A*, using ts *cfd1* cells and *ScCFD1* as a positive control.

Next, we investigated whether AtNBP35 can replace the function of yeast Nbp35 using cells carrying a temperature-sensitive mutant copy of the endogenous *NBP35* gene (32, 33). Upon shifting the cells to 37 °C, the mutant ScNbp35 protein becomes non-functional, leading to growth arrest after a few cell duplications. The growth of the temperature-shifted *nbp35* mutant was rescued by expression of wild-type *ScNBP35* from a plasmid but not by *Arabidopsis NBP35* (Fig. 6). We then tested whether *AtNBP35* could rescue a temperature-sensitive *cfd1* mutant (33). Surprisingly, expression of *AtNBP35* enabled slow growth of temperature-sensitive *cfd1* mutant cells shifted to 37 °C. We also tested the functional requirement of the N-terminal domain of AtNBP35 for yeast complementation, as yeast Cfd1 lacks this domain. Truncated ΔN AtNBP35 did not complement the temperature-sensitive *cfd1* mutant, although the protein was stably expressed (supplemental Fig. S2). Similar results were obtained with galactose-regulatable mutants of *NBP35* and *CFD1* (not shown). In summary, AtNBP35 is able to acquire Fe-S cofactors in the yeast cytosol but cannot substitute for the endogenous yeast Nbp35. In contrast, AtNBP35 can partially replace the function of Cfd1 in yeast.

AtNBP35 Is Ubiquitously Expressed and Essential for Embryo Development—To assess the role of NBP35 in *Arabidopsis*, we investigated the expression of *AtNBP35* and analyzed available insertion mutants. Immunoblot analysis of vegetative and reproductive organs showed that *AtNBP35* is ubiquitously expressed (Fig. 7*A*). This is in agreement with microarray data from the GeneVestigator data base (supplemental Fig. S4). Comparison of the signal intensities in lanes with cell extract and known amounts of purified protein indicated that the abundance of AtNBP35 is less than 0.005% of SDS-extractable protein.

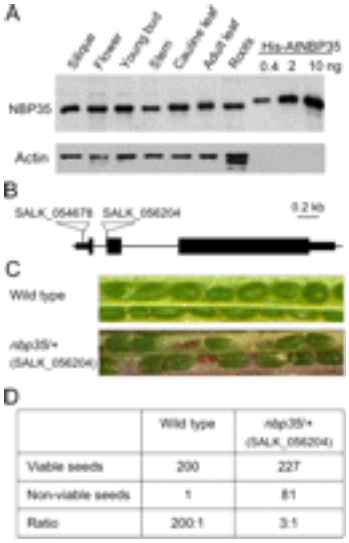

View larger version:

In this page In a new window

Download as PowerPoint Slide

FIGURE 7.

***AtNBP35* is universally expressed and essential for embryo development.** *A*, expression of *AtNBP35* in different plant organs. Proteins were extracted in buffer containing 1% (w/v) SDS, centrifuged, and subjected to immunoblotting with antibodies against AtNBP35 (30 μg of protein per lane). Antibodies against actin served as a loading control (*lower panel*). Purified His-tagged AtNBP35 (0.4–10 ng) was used to estimate the abundance of AtNBP35 in cell extracts (*three right lanes*). *B*, gene structure of *AtNBP35* (At5g50960) showing the positions of the T-DNA inserts in the SALK lines. *kb*, kilobases. *C*, seed set in wild type and a heterozygote *atnbp35 Arabidopsis* line (SALK_056204). *D*, genetic analysis of the heterozygous T-DNA line. One quarter of the seeds of the heterozygous *atnbp35*/+ line do not develop and are unviable, corresponding to the expected number of homozygous (-/-) segregants.

Two plant lines with insertions in the *AtNBP35* gene were obtained from the *Arabidopsis* stock center. SALK_054678 contains a T-DNA insert in the 5′-untranslated region, and SALK_056204 contains a T-DNA insert at the 3′ end of the first intron (Fig. 7*B*). Homozygous plants were bred from the SALK_054678 line, but they had no detectable phenotype. Reverse transcription PCR using primers in the 5′- and 3′-untranslated region confirmed the absence of full-length NBP35 transcript (not shown). However, PCR products covering the start and end of the coding sequence were as abundant as in wild type, suggesting that an alternative transcription start site was used to produce sufficient amounts of functional *AtNBP35* mRNA. In contrast, no homozygous plants were obtained from the SALK_056204 line. PCR analysis indicated that transcript levels were decreased by half in heterozygous plants (not shown). Closer examination of the siliques of these plants revealed that a quarter of the seeds were not properly developed, appearing small and dark brown (Fig. 7*C*). The ratio of underdeveloped to normal seeds was 1:3 (Fig. 7*D*), indicating that the mutation is recessive, that is, those embryos with at least one copy of the functional *AtNBP35* gene survive. The requirement of *AtNBP35* for embryo development together with its constitutive expression indicate that NBP35 performs an essential function in the plant cell.

Previous Section
Next Section

DISCUSSION

In plants and algae, Fe-S proteins are abundant in four cell compartments: plastids, mitochondria, cytosol, and nucleus. Biogenesis of Fe-S proteins in the latter two compartments has not been investigated in photosynthetic organisms despite the occurrence of unique and important Fe-S proteins. It has been proposed that in mammals alternative splicing mechanisms provide small

amounts of ISC protein isoforms in the cytosol. However, localization data of various ISC proteins in *Arabidopsis* argue against this possibility in plants (23, 34, 35). Moreover, recent reports in mammals show that cytosolic Fe-S protein assembly is dependent on the mitochondrial ISC machinery rather than the cytosolic ISC isoforms (36, 37). In addition, the CIA machinery is required for Fe-S protein assembly in the cytosol of human cell lines (12, 38). We have, therefore, started to functionally analyze plant homologs of the CIA proteins using a reverse genetics approach. Focusing on two uncharacterized Mrp-like proteins in the model plant *Arabidopsis*, we showed that a homolog of one of the yeast CIA proteins, AtNBP35, is present in the plant cytosol (Fig. 2). In contrast, a Cfd1-type partner protein as found in fungi and Metazoa (11, 12) could not be identified either as a separate protein coding sequence in any of the sequenced plant or algal genomes or as a cytosolic isoform of the mitochondrial INDL protein in *Arabidopsis* (Fig. 2).

Another marked difference between plant/algal and the fungal/metazoan NBP35 proteins is the absence of the C-terminal C*XX*C motif, which is replaced by an ~35-amino acid insertion in the plant/algal proteins. This change may have occurred early in the evolution of the Viridiplantae, as it is found across the green lineage (plants and green algae) but not in the rhodophyte (red alga) *Cyanidioschyzon merolae* (39) (supplemental Fig. S1). The *C. merolae* genome also encodes HCF101 and INDL but not a CFD1 protein. Thus, the NBP35 protein in *C. merolae* may represent the ancestral form containing the C-terminal C*XX*C motif but no CFD1 partner. Hence, one might speculate that CFD1 may have arisen as a consequence of gene duplication in the fungal/metazoan group.

Despite the lack of the characteristic C*XX*C motif, the C-terminal domain of AtNBP35 bound an Fe-S cluster upon chemical reconstitution (Fig. 3). It will be interesting, therefore, to investigate more precisely the role of the C*XX*C motif in the function of the Mrp-like proteins, as this motif is also absent in HCF101. In contrast, mutation studies have shown that the individual cysteines of the C*XX*C motif in yeast Cfd1 and Yarrowia Ind1 are essential (10, 16). Quantification of bound Fe and sulfide in reconstituted AtNBP35 suggested that the C-terminal [4Fe-4S] cluster was shared between two protomers. A similar situation has been proposed for the bacterial Mrp-like protein called ApbC in *Salmonella enterica* (40). As a consequence, each polypeptide would provide two ligands to this cluster which remain to be determined by site-directed mutagenesis. The presence of the C-terminal cluster is not required for dimer formation, as the as-isolated FL protein was able to form dimers (Fig. 3, *A* and *B*).

To initiate the functional analysis of AtNBP35, we performed an *in vitro* cluster transfer assay and complementation studies with yeast *nbp35* and *cfd1* mutants. Although the *in vitro* assay suggested similar cluster transfer properties of AtNBP35 and ScNbp35 (Fig. 4 and Ref. 11), expression of *AtNBP35* could not rescue the growth defect of ScNbp35-depleted cells (Fig. 6). The reason for the lack of complementation is not known; Fe-S cluster assembly on AtNBP35 could be demonstrated in yeast, and control experiments confirmed stable expression of AtNBP35 in the yeast cytosol (Fig. 5). Surprisingly, the growth of ScCfd1-depleted cells was restored albeit partially by expression of FL *AtNBP35* but not without the N-terminal domain.

Our studies presented here will be fundamental for further studies to unravel the precise molecular function of *AtNBP35.* Because we have shown that *AtNBP35* is an essential gene (Fig. 7), embryo lethality has to be circumvented by the construction of partial or regulatable knock-down mutants, which is in progress in our laboratory. Moreover, it will be interesting to investigate the cellular role of other CIA homologs in plants, including AtNAR1 (41) and AtCIA1 (42), and to study their protein interactions with AtNBP35. The presence of NBP35 as a homooligomer in the plant cytosol rather than the Cfd1-Nbp35 complex shows that plants provide an insightful model system for Fe-S protein biogenesis and the compartmentalization of this process in eukaryotic cells.

Previous Section
Next Section

Acknowledgments

We thank Stéphane Lobréaux for the AtISU1 antibodies, John C. Gray for the PETC antibodies, and Rudolf K. Thauer (Max Planck Institute, Marburg) for access to the EPR spectrometer.

Previous Section
Next Section

Footnotes

↵3 The abbreviations used are: ISC, iron-sulfur cluster (assembly); At, *A. thaliana*; CIA, cytosolic iron-sulfur cluster assembly; FL, full-length; GFP, green fluorescent protein; ΔN, deletion of N-terminal domain; NBP, nucleotide binding protein; Sc, *S. cerevisiae*.

↵4 D. J. A. Netz, unpublished information.

↵* This research was funded by the Royal Society (to J. B.), the Danish Research Agency and the Carlsberg Foundation (to K. B.), Ministero dell'Istruzione, dell'Università e della Ricerca (to G. V.), Deutsche Forschungsgemeinschaft (SFB 593 and TR1, Gottfried-Wilhelm Leibniz Programm, and GRK 1216), and Fonds der Chemischen Industrie (to R. L.). The costs of publication of this article were defrayed in part by the payment of page charges. This article must therefore be hereby marked "*advertisement*" in accordance with 18 U.S.C. Section 1734 solely to indicate this fact.

↵ The on-line version of this article (available at http://www.jbc.org) contains supplemental Figs. S1–S4.

↵1 Current address: Dipartimento di Produzione Vegetale, University of Milano, Via Celoria 2, I-20133 Milano, Italy.

Received September 22, 2008.
Revision received October 24, 2008.

Previous Section

References

1 ↵ Beinert, H. (2000) *J. Biol. Inorg. Chem.* **5**, 2-15 **CrossRefMedlineGoogle Scholar**
2 ↵ Johnson, D. C., Dean, D. R., Smith, A. D., and Johnson, M. K. (2005) *Annu. Rev. Biochem.* **74**, 247-281 **CrossRefMedlineGoogle Scholar**
3 ↵ Lill, R., and Mühlenhoff, U. (2008) *Annu. Rev. Biochem.* **77**, 669-700 **CrossRefMedlineGoogle Scholar**
4 ↵ Balk, J., and Lobréaux, S. (2005) *Trends Plant Sci.* **10**, 324-331 **CrossRefMedlineGoogle Scholar**
5 Kessler, D., and Papenbrock, J. (2005) *Photosynth. Res.* **86**, 391-407 **CrossRefMedlineGoogle Scholar**
6 ↵ Pilon, M., Abdel-Ghany, S. E., Van Hoewyk, D., Ye, H., and Pilon-Smits, E. A. (2006) *Genet. Eng.* **27**, 101-117 **CrossRefGoogle Scholar**
7 ↵ Hirata, A., Klein, B. J., and Murakami, K. S. (2008) *Nature* **451**, 851-854 **CrossRefMedlineGoogle Scholar**
8 ↵ Godman, J., and Balk, J. (2008) *Genetics* **179**, 59-68 Abstract/FREE Full Text
9 ↵ Hausmann, A., Aguilar Netz, D. J., Balk, J., Pierik, A. J., Mühlenhoff, U., and Lill, R. (2005) *Proc. Natl. Acad. Sci. U. S. A.* **102**, 3266-3271 Abstract/FREE Full Text
10 ↵ Roy, A., Solodovnikova, N., Nicholson, T., Antholine, W., and Walden, W. E. (2003) *EMBO J.* **22**, 4826-4835 **CrossRefMedlineGoogle Scholar**
11 ↵ Netz, D. J., Pierik, A. J., Stümpfig, M., Mühlenhoff, U., and Lill, R. (2007) *Nat. Chem. Biol.* **3**, 278-286 **CrossRefMedlineGoogle Scholar**
12 ↵ Stehling, O., Netz, D. J., Niggemeyer, B., Rösser, R., Eisenstein, R. S., Puccio, H., Pierik, A. J., and Lill, R. (2008) *Mol. Cell. Biol.* **28**, 5517-5528 Abstract/FREE Full Text
13 ↵ Leipe, D. D., Koonin, E. V., and Aravind, L. (2002) *J. Mol. Biol.* **333**, 781-815 **Google Scholar**
14 ↵ Lezhneva, L., Amann, K., and Meurer, J. (2004) *Plant J.* **37**, 174-185 **MedlineGoogle Scholar**
15 ↵ Stöckel, J., and Oelmüller, R. (2004) *J. Biol. Chem.* **279**, 10243-10251 Abstract/FREE Full Text

16 ↵ Bych, K., Kerscher, S., Netz, D. J., Pierik, A. J., Zwicker, K., Huynen, M. A., Lill, R., Brandt, U., and Balk, J. (2008) *EMBO J.* **27**, 1736-1746 **CrossRefMedlineGoogle Scholar**
17 ↵ Prime, T. A., Sherrier, D. J., Mahon, P., Packman, L. C., and Dupree, P. (2000) *Electrophoresis* **21**, 3488-3499 **CrossRefMedlineGoogle Scholar**
18 ↵ Kispal, G., Csere, P., Prohl, C., and Lill, R. (1999) *EMBO J.* **18**, 3981-3989 **CrossRefMedlineGoogle Scholar**
19 ↵ Mumberg, D., Müller, R., and Funk, M. (1995) *Gene (Amst.)* **156**, 119-122 **CrossRefMedlineGoogle Scholar**
20 ↵ Sweetlove, L. J., Taylor, N. L., and Leaver, C. J. (2007) *Methods Mol. Biol.* **372**, 125-136 **CrossRefMedlineGoogle Scholar**
21 ↵ Balk, J., Chew, S. K., Leaver, C. J., and McCabe, P. F. (2003) *Plant J.* **34**, 573-583 **CrossRefMedlineGoogle Scholar**
22 ↵ Aronsson, H., and Jarvis, P. (2002) *FEBS Lett.* **529**, 215-220 **CrossRefMedlineGoogle Scholar**
23 ↵ Léon, S., Touraine, B., Briat, J.-F., and Lobréaux, S. (2005) *FEBS Lett.* **579**, 1930-1934 **CrossRefMedlineGoogle Scholar**
24 ↵ Salter, A. H., Newman, B. J., Napier, J. A., and Gray, J. C. (1992) *Plant Mol. Biol.* **20**, 569-574 **CrossRefMedlineGoogle Scholar**
25 ↵ Balk, J., Pierik, A. J., Netz, D. J., Mühlenhoff, U., and Lill, R. (2004) *EMBO J.* **23**, 2105-2115 **CrossRefMedlineGoogle Scholar**
26 ↵ Barthelme, D., Scheele, U., Dinkelaker, S., Janoschka, A., MacMillan, F., Albers, S.-V., Driessen, A. J. M., Stagni, M. S., Bill, E., Meyer-Klaucke, W., Schümann, V., and Tampé, R. (2007) *J. Biol. Chem.* **282**, 14598-14607 Abstract/FREE Full Text
27 ↵ Peeters, N. M., Chapron, A., Giritch, A., Grandjean, O., Lancelin, D., Lhomme, T., Vivrel, A., and Small, I. (2000) *J. Mol. Evol.* **50**, 413-423 **MedlineGoogle Scholar**
28 ↵ von Arnim, A. G., Deng, X.-W., and Stacey, M. G. (1998) *Gene (Amst.)* **221**, 35-43 **CrossRefMedlineGoogle Scholar**
29 ↵ Seibel, N. M., Eljouni, J., Nalaskowski, M. M., and Hampe, W. (2007) *Anal. Biochem.* **368**, 95-99 **CrossRefMedlineGoogle Scholar**
30 ↵ Orme-Johnson, W. H., and Orme-Johnson, A. R. (1982) in *Iron-Sulfur Proteins* (Spiro, T. G., ed) pp. 67-95, John Wiley & Sons, Inc., New York **Google Scholar**
31 ↵ Ferreira, G. C., Franco, R., Lloyd, S. G., Pereira, A. S., Moura, I., Moura, J. J. G., and Huynh, B. H. (1994) *J. Biol. Chem.* **269**, 7062-7065 Abstract/FREE Full Text
32 ↵ Vitale, G., Fabre, E., and Hurt, E. C. (1996) *Gene (Amst.)* **178**, 97-106 **CrossRefMedlineGoogle Scholar**
33 ↵ Yarunin, A., Panse, V. G., Petfalski, E., Dez, C., Tollervey, D., and Hurt, E. C. (2005) *EMBO J.* **24**, 580-588 **CrossRefMedlineGoogle Scholar**
34 ↵ Kushnir, S., Babiychuk, E., Storozhenko, S., Davey, M. W., Papenbrock, J., De Rycke, R., Engler, G., Stephan, U. W., Lange, H., Kispal, G., Lill, R., and Van Montagu, M. (2001) *Plant Cell* **13**, 89-100 Abstract/FREE Full Text
35 ↵ Frazzon, A. P., Ramirez, M. V., Warek, U., Balk, J., Frazzon, J., Dean, D. R., and Winkel, B. S. (2007) *Plant Mol. Biol.* **64**, 225-240 **CrossRefMedlineGoogle Scholar**
36 ↵ Tong, W. H., and Rouault, T. A. (2006) *Cell Metab.* **3**, 199-210 **CrossRefMedlineGoogle Scholar**
37 ↵ Biederbick, A., Stehling, O., Rösser, R., Niggemeyer, B., Nakai, Y., Elsässer, H. P., and Lill, R. (2006) *Mol. Cell. Biol.* **26**, 5675-5687 Abstract/FREE Full Text
38 ↵ Song, D., and Lee, F. S. (2008) *J. Biol. Chem.* **283**, 9231-9238 Abstract/FREE Full Text
39 ↵ Matsuzaki, M., Misumi, O., Shin-I, T., Maruyama, S., Takahara, M., Miyagishima, S. Y., Mori, T., Nishida, K., Yagisawa, F., Nishida, K., Yoshida, Y., Nishimura, Y., Nakao, S., Kobayashi, T., Momoyama, Y., Higashiyama, T., Minoda, A., Sano, M., Nomoto, H., Oishi, K., Hayashi, H., Ohta, F., Nishizaka, S., Haga, S., Miura, S., Morishita, T., Kabeya, Y., Terasawa, K., Suzuki, Y., Ishii, Y., Asakawa, S., Takano, H., Ohta, N., Kuroiwa, H., Tanaka,

K., Shimizu, N., Sugano, S., Sato, N., Nozaki, H., Ogasawara, N., Kohara, Y., and Kuroiwa, T. (2004) *Nature* **428**, 653-657 **CrossRefMedlineGoogle Scholar**

40 ↵ Boyd, J. M., Pierik, A. J., Netz, D. J., Lill, R., and Downs, D. M. (2008) *Biochemistry* **47**, 8195-8202 **CrossRefMedlineGoogle Scholar**

41 ↵ Cavazza, C., Martin, L., Mondy, S., Gaillard, J., Ratet, P., and Fontecilla-Camps, J. C. (2008) *J. Inorg. Biochem.* **102**, 1359-1365 **CrossRefMedlineGoogle Scholar**

42 ↵ Balk, J., Aguilar Netz, D. J., Tepper, K., Pierik, A. J., and Lill, R. (2005) *Mol. Cell. Biol.* **25**, 10833-10841 Abstract/FREE Full Text

-